Journal of Scientific Computing (2020) 82:19
https://doi.org/10.1007/s10915-020-01123-1

A Homotopy Method with Adaptive Basis Selection for Computing Multiple Solutions of Differential Equations

Wenrui Hao[1] · Jan Hesthaven[2] · Guang Lin[3] · Bin Zheng[4]

Received: 12 February 2019 / Revised: 18 October 2019 / Accepted: 2 January 2020 /
Published online: 13 January 2020

Abstract
The homotopy continuation method has been widely used to compute multiple solutions of nonlinear differential equations, but the computational cost grows exponentially based on the traditional finite difference and finite element discretizations. In this work, we presented a new method by constructing a spectral approximation space adaptively based on a greedy algorithm for nonlinear differential equations. Then multiple solutions were computed by the homotopy continuation method on this low-dimensional approximation space. Various numerical examples were given to illustrate the feasibility and the efficiency of this new approach.

Keywords Multiple solutions · Nonlinear differential equations · Polynomial systems · Homotopy continuation

1 Introduction

Many mathematical models of natural phenomena, e.g., biology [18,19], physics [35,36] and materials science [38], involve nonlinear systems of partial differential equations (PDEs) [21, 22,30,31,33]. Theories and numerical methods for these nonlinear PDEs have been developed

✉ Bin Zheng
binzhengmath@gmail.com

Wenrui Hao
wxh64@psu.edu

Jan Hesthaven
Jan.Hesthaven@epfl.ch

Guang Lin
guanglin@purdue.edu

1 Department of Mathematics, Pennsylvania State University, University Park, PA 16802, USA

2 Computational Mathematics and Simulation Science, École Polytechnique Fédérale de Lausanne, 1015 Lausanne, Switzerland

3 Department of Mathematics, Purdue University, West Lafayette, IN 47907, USA

4 Beijing Institute for Scientific and Engineering Computing, Beijing University of Technology, Beijing 100124, China

to gain a better understanding of the solution structures, in which bifurcations [46–49] and multiple steady states [8,11,17,26,27,33,37] are the central questions [29,57]. Although PDE theory can help us understand the solution structures in many cases [20,23–25], the in-depth and more quantitative study of these problems often requires numerically computing multiple steady-state solutions. Traditional numerical methods [43,53] focus on the unique time-marching solution and are very hard to capture multiple solutions [46,47] and the structural stability [48,49].

In order to address these challenges, homotopy continuation methods [39–42] have been developed for computing multiple solutions, steady-states, and bifurcation diagrams of nonlinear PDEs [32,33]. These numerical methods show significant advantages in handling nonlinear parametric PDEs and have been applied to hyperbolic conservation laws [34], physical systems [35,36], and some more complex free boundary problems arising from biology [30,31]. In practice, this approach may be computationally intensive due to the rapid growth of the number of solutions when refining the mesh [2]. To address this difficulty, the *filtering method* has been introduced to limit the number of paths to be followed at each step for solving the nonlinear boundary value problem in one dimension [1] and semilinear elliptic equations in two dimensions [2]. Another strategy for adapting homotopy continuation method to solve PDE problems is the so-called *bootstrapping method*, which uses domain decomposition to break the large polynomial system into small ones and track the solutions back to the original system [33]. However, the computational cost for both methods grows dramatically when the number of mesh points increases. Furthermore, the stopping criteria and filtering conditions are constructed case by case.

The reduced basis method (RBM) has been widely used for solving parametric PDEs [15,16,28,50,51,59]. The basic idea of RBM is to construct a very low-dimensional approximation space by the span of solutions corresponding to properly selected parameter values (usually by a greedy algorithm), and then to use Galerkin projection to find solutions corresponding to new parameter values in this approximation space. Motivated by the RBM, in this paper, we developed a spectral discretization to reduce the size of the discretized polynomial system by selecting basis functions (which are polynomials) of the spectral discretization adaptively by a greedy algorithm. More specifically, we constructed an approximation space of very low dimension for approximating nonlinear PDEs which, in turn, reduces the size of the discrete polynomial systems significantly. This adaptive approach is able to reduce the computational complexity significantly when combined with the homotopy continuation method to solve the discretized polynomial systems.

The rest of this paper is organized as follows. We first gave a brief overview of numerical methods for computing multiple solutions of nonlinear PDEs in Sect. 2. In Sect. 3, we presented the details of the homotopy method with adaptive basis selection (HMABS) for computing multiple solutions of nonlinear differential equations. Then, we discussed the convergence analysis of the HMABS in Sect. 4. Finally, several numerical examples were given in Sect. 5 to demonstrate the accuracy and efficiency of the HMABS approach.

2 Homotopy Continuation Methods for Solving Nonlinear Differential Equations

In this section, we briefly review existing homotopy continuation approaches for computing multiple solutions of nonlinear differential equations. Based on the finite difference method, the homotopy continuation method has been developed for solving the discretized polyno-

mial systems [2], which is based on numerical techniques arising from numerical algebraic geometry [5,56].

2.1 Homotopy Continuation Method

We consider a finite difference discretization of a differential equations with an uniform mesh, namely, approximate a solution u by an n-tuple $\boldsymbol{U} = (U_1, U_2, \ldots, U_n) \in \mathbb{R}^n$ where n is the number of grid points. Then the resulting discretization polynomial system is denoted as

$$F_h(\boldsymbol{U}) = 0, \tag{1}$$

where h is the mesh size (i.e., $h = (b-a)/(n+1)$ with domain $\Omega = (a, b)$). To solve (1) by the homotopy continuation method, we first define the following homotopy function

$$H(\boldsymbol{U}, t) = F_h(\boldsymbol{U})(1-t) + \gamma t S(\boldsymbol{U}) = 0, \tag{2}$$

where γ is a randomly chosen complex number and $t \in [0, 1]$ is the path tracking parameter. Here $S(\boldsymbol{U})$ is the start system defined by

$$S(\boldsymbol{U}) = \begin{pmatrix} U_1^k - 1 \\ \vdots \\ U_n^k - 1 \end{pmatrix} = 0$$

where k is the degree of each polynomial in $F_h(\boldsymbol{U})$. When $t = 1$, $H(\boldsymbol{U}, 1) = S(\boldsymbol{U}) = 0$ can be solved for each U_i separately on the complex field. Although that the numerical solutions of (2) are real, we have to track all the complex solutions of the start system in order to guarantee all the real solutions of (2). Then the polynomial systems (2) is solved by tracking t from 1 to 0. For a more detailed description of the numerical continuation method for multiple solutions of differential equations, we refer the reader to [1–4]. However, the computation cost of homotopy method is $O(k^n)$ therefore it is hard to solve a discretized polynomial system based on a fine mesh.

2.2 Bootstrapping Method

The bootstrapping method [33], coupling homotopy and domain decomposition methods, computes multiple solutions of nonlinear differential equation systems with natural parallelizability. This approach shows that domain decomposition gives excellent guidance on how to choose smaller systems to build up to a larger system. The basic idea of bootstrapping method is to first use homotopy continuation to compute all solutions to the discretized polynomial system $F_H(\boldsymbol{U}) = 0$ with a coarse grid of size H, and then using the solutions as "boundary conditions" of subdomain systems, i.e., solve the hybrid system $F_{h,H}(\boldsymbol{U}) = 0$ ($h = H/m$ where m is the number of grid points on each subdomain). Then, solutions of the discretized polynomial system $F_h(\boldsymbol{U}) = 0$ with the fine grid of size h are computed through the following homotopy:

$$\mathcal{H}(\boldsymbol{u}, t) = (1-t)F_h(\boldsymbol{U}) + tF_{h,H}(\boldsymbol{U}) \tag{3}$$

where t is the homotopy parameter. When $t = 1$, solutions of the hybrid system $F_{h,H}(\boldsymbol{U}) = 0$ are solved based on the domain decomposition setup. Thus as tracking t from 1 to 0, the

solutions on the fine grid will be obtained. Full details of the bootstrapping method can be found in [33].

The bootstrapping method, which naturally couples domain decomposition with homotopy continuation methods, allows us to solve the discretized polynomial system on the complex field to obtain multiple solutions. Nevertheless, recovering the full system on the fine grid from subsystems on the coarse grid is time-consuming. The reason is that the size of the full discretized polynomial system is too large to track on the complex field although each subdiscretized polynomial system is small to solve easily. To address this difficulty, we choose the spectral Galerkin method to discretize nonlinear differential equations which usually result in polynomial systems with a smaller size. In fact, the advantage of the spectral discretization is to obtain accurate numerical solutions by using a relatively low-dimensional approximation space [52]. This low dimensionality in turn reduces the size of the discretized polynomial systems which can be solved more efficiently by the homotopy continuation method.

3 Homotopy Method with Adaptive Basis Selection

3.1 Model Problem and Spectral Galerkin Discretization

We consider the following semilinear elliptic equation with a homogeneous Dirichlet boundary condition:

$$\begin{cases} -\Delta u = f(u), & \text{in } \Omega \\ u = 0, & \text{on } \partial\Omega, \end{cases} \tag{4}$$

where $\Omega \subset \mathbb{R}^d$ is an open bounded domain in d dimension and $f(u)$ is a polynomial function of u. The weak formulation of problem (4) is: seek $u \in H_0^1(\Omega)$ such that

$$F(u, v) := (A(u), v) = (\nabla u, \nabla v) - (f(u), v) = 0, \ \forall v \in H_0^1(\Omega), \tag{5}$$

where $(\cdot, \cdot)$ is the usual L^2 inner product. The Galerkin discretization of (5) is: find $u_{\mathcal{N}} \in V_{\mathcal{N}}$ such that

$$F(u_{\mathcal{N}}, v) = 0, \quad \forall v \in V_{\mathcal{N}}, \tag{6}$$

where $V_{\mathcal{N}} \subset H_0^1(\Omega)$ is a finite dimensional approximation space spanned by a set of basis functions $\{\phi_i\}_{i=1}^{\mathcal{N}}$. For spectral Galerkin method using the Legendre polynomials, $V_{\mathcal{N}}$ is composed of polynomial functions of degree k. Let us denote the numerical approximation by

$$u_{\mathcal{N}} = \sum_{j=1}^{\mathcal{N}} \alpha_j \phi_j. \tag{7}$$

The discrete problem (6) is equivalent to a system of $\mathcal{N}$ polynomial equations with respect to the unknown coefficients $\boldsymbol{\alpha} = (\alpha_1, \ldots, \alpha_{\mathcal{N}})$,

$$G_{\mathcal{N},i}(\boldsymbol{\alpha}) := F\left(\sum_{j=1}^{\mathcal{N}} \alpha_j \phi_j, \phi_i\right) = 0, \quad i = 1, \ldots, \mathcal{N}. \tag{8}$$

Remark 1 Our method is based on the polynomial basis satisfying given boundary conditions which have been constructed by using Legendre polynomials in [14]. When the domain has

an irregular boundary or the boundary conditions are complicated, we can use the finite element method to compute basis functions first and then expand the solution by Galerkin projection.

3.2 Adaptive Basis Selection

In order to reduce the size of the discrete polynomial system (8), we will choose an optimal set of basis functions for the approximation space. By denoting a set of basis functions of $V_{\mathcal{N}}$ as $\{\phi_i\}_{i=1}^{\mathcal{N}}$, we construct the following nested sequence of approximation spaces $V_1 \subset V_2 \subset \cdots \subset V_{\mathcal{N}}$, where $V_l = \text{span}\{V_{l-1} \cup \phi_{\mathcal{I}_l}\}$, $\phi_{\mathcal{I}_l}$ is a basis function with index $\mathcal{I}_l$ ($l = 1, \ldots, \mathcal{N}$) determined by a greedy sampling strategy based on the a posteriori error estimator

$$E_l(\phi_j) := |F\left(u_l, \phi_j\right)| \ (j = 1, \ldots, \mathcal{N}).$$

Here $u_l := \sum_{i=1}^{l} \alpha_i \phi_{\mathcal{I}_i}$ is a solution of the nonlinear polynomial system $\mathbf{G}_l = (G_{l,1}, \ldots, G_{l,l})$ with

$$G_{l,j}(\alpha_1, \ldots, \alpha_l) := F\left(\sum_{i=1}^{l} \alpha_i \phi_{\mathcal{I}_i}, \phi_{\mathcal{I}_j}\right) = 0, \quad j = 1, \ldots, l. \tag{9}$$

Since $\mathbf{G}_l$ corresponds to a polynomial system, there could be multiple solutions for $\boldsymbol{\alpha} = (\alpha_1, \ldots, \alpha_l)$. Thus, we use $u_l^{(p)}$ ($p = 1, \ldots, S$, where S is the number of solutions) to denote these different solutions. Then, we choose

$$\mathcal{I}_{l+1} := \arg\max_{1 \le j \le \mathcal{N}} \sum_{p=1}^{S} |F(u_l^{(p)}, \phi_j)|. \tag{10}$$

The above process is terminated if for a prescribed tolerance ε, we have

$$\sum_{p=1}^{S} |F(u_l^{(p)}, \phi_{\mathcal{I}_{l+1}})| < \varepsilon. \tag{11}$$

Otherwise, set $V_{l+1} = \text{span}\{V_l \cup \phi_{\mathcal{I}_{l+1}}\}$, and repeat the above process to construct the next approximation space V_{l+2}. Then the detailed algorithm is outlined in Algorithm 1.

Algorithm 1: A greedy algorithm for constructing the approximation space

Input : Candidate basis function $\{\phi_i\}_{i=1}^{\mathcal{N}}$, bilinear form $F(u, v)$, and stopping tolerance ε.
Initialization: $\phi_{\mathcal{I}_1} = \phi_1$, $V_1 = \text{span}\{\phi_{\mathcal{I}_1}\}$.
for $l = 1 : \mathcal{N}$ **do**
- solve the nonlinear system $\mathbf{G}_l(\boldsymbol{\alpha}) = \mathbf{0}$;
- choose $\mathcal{I}_{l+1} = \arg\max_{1 \le j \le \mathcal{N}} \sum_{p=1}^{S} |F(u_l^{(p)}, \phi_j)|$;
- **if** $\sum_{p=1}^{S} |F(u_l^{(p)}, \phi_{\mathcal{I}_{l+1}})| < \varepsilon$ **then**
  break
  end
- $V_{l+1} = \text{span}\{V_l \cup \phi_{\mathcal{I}_{l+1}}\}$.

end

Remark 2 Notice that the size of the nonlinear system (9) equals l which is typically very small compared with (8). Thus the homotopy continuation method is efficient in computing

all the complex solutions. In addition, the residual computations can be parallelized to further increase the efficiency of the above algorithm.

3.3 Homotopy Method for Solving the Discretized Polynomial System

In order to compute solutions of $\mathbf{G}_{l+1}(\boldsymbol{\alpha}) = \mathbf{0}$, we define the following homotopy function:

$$\mathbf{H}(\boldsymbol{\alpha}, t) = \begin{bmatrix} \mathbf{G}_{l+1}(\alpha_1, \ldots, \alpha_{l+1}) \\ \tilde{\alpha}_1 - \alpha_1 \\ \vdots \\ \tilde{\alpha}_l - \alpha_l \end{bmatrix} (1-t) + \gamma t \begin{bmatrix} \mathbf{G}_l(\alpha_1, \ldots, \alpha_l) \\ F(\tilde{u}_l, \phi_{\mathcal{I}_{l+1}}; \widetilde{\alpha_1}, \ldots, \widetilde{\alpha_l}) \end{bmatrix} = \mathbf{0}, \tag{12}$$

where γ is a randomly chosen complex number to avoid singularities during the homotopy tracking t from 1 to 0 which is called the γ-trick [5,56]. Here $\tilde{u}_l = \sum_{i=1}^{l} \tilde{\alpha}_i \phi_{\mathcal{I}_i} + \alpha_{l+1}\phi_{\mathcal{I}_{l+1}}$, and $\widetilde{\alpha}_i$ are random complex numbers. Then the start system $H(\boldsymbol{\alpha}, 1)$ can be decoupled into two systems: $\mathbf{G}_l(\alpha_1, \ldots, \alpha_l) = \mathbf{0}$ which has been solved in the previous step; $F(\tilde{u}_l, \phi_{\mathcal{I}_{l+1}}; \widetilde{\alpha_1}, \ldots, \widetilde{\alpha_l}) = 0$ (defined in (6)) which is solved for α_{l+1} as the single variable while $\tilde{\alpha}_i$ are given random complex numbers. The solutions of the start system are hybrid: all the real solutions from $\mathbf{G}_l(\cdot) = 0$ and all the complex solutions of the new added equation $F(\cdot) = 0$. This choice might miss some solutions of $\mathbf{G}_{l+1}(\cdot) = 0$ since we choose the real solutions only for $\mathbf{G}_l(\cdot) = 0$. However, this choice reduces the computation significantly and only real solutions are meaningful for $\mathbf{G}_{l+1}(\cdot) = 0$. Then, this homotopy $\mathbf{H}(\boldsymbol{\alpha}, t)$ can efficiently solve $\mathbf{G}_{l+1}(\alpha_1, \ldots, \alpha_{l+1}) = \mathbf{0}$ by lifting $l+1$ variables to $2l+1$ variables. This homotopy setup is so called the diagonal homotopy which has been used for computing proper lifts of intersections of algebraic sets (see [54,55] for more details). Moreover, this homotopy method can be combined with adaptive stepsize and adaptive precision algorithms [3,6] to provide reliability and efficiency.

Finally, we summarized the HMABS approach for computing multiple solutions of differential equations as follows:

- choosing the candidate basis to form a complete normalized base of the Sobolev space $H_0^1\{\Omega\}$;
- expanding the optimal basis space based on **Algorithm** 1;
- solving the discretized polynomial system $\mathbf{G}_{l+1}() = \mathbf{0}$ by the homotopy setup in Eq. (12).

4 Convergence Analysis

In this section we will prove the convergence of the HMABS approach for a single solution case while the convergence for multiple solutions will be explored in the future since it will involve other advanced techniques.

We assume that the nonlinear variational problem (5) has a solution u such that the Fréchet derivative at the point u (denoted by $DF(u)$) is an isomorphism from $H_0^1(\Omega)$ to $H^{-1}(\Omega)$ which implies that u is an isolated solution. We find u by using Newton iteration. Starting from an initial approximation u^0 ($\approx u$), we solve for $w \in H_0^1$ such that

$$< DF(u^k)w, v >= -F(u^k, v), \ \forall\, v \in H_0^1(\Omega), \tag{13}$$

and set $u^{k+1} = u^k + w$. The linearized operator $DF(u) : H_0^1(\Omega) \to H^{-1}(\Omega)$ given by $DF(u)w = -\Delta w - Df(u)w$ satisfies

$$< DF(u)w, v >= (Df(u)w, v) - (\nabla w, \nabla v). \tag{14}$$

The well-posedness of the linearized problem (13) follows from the coercivity and boundedness assumptions on DF and F.

For the discrete problem (6), following the general framework in [45,60], and the convergence estimate for the greedy algorithm [10], we have the following estimate.

Theorem 1 *Let u be an isolated solution of the nonlinear problem (5), $V_{\mathcal{N}}$ the approximation space of dimension $\mathcal{N}$, and $\tilde{u}_{\mathcal{N}}$ the approximated solution by the HMABS method. Assuming $DF(u)$ is Lipschitz continuous in a neighborhood of u, for some constants $\beta_{\mathcal{N}}$ and η, we have*

$$\|u - \tilde{u}_{\mathcal{N}}\|_1 \leq C\beta_{\mathcal{N}}^{-1} \inf_{w \in V_{\mathcal{N}}} \|u - w\|_1 + Ce^{-\eta N}, \tag{15}$$

where N is the dimension of the approximation space obtained by the greedy Algorithm 1.

Proof Let $u_{\mathcal{N}}$ be the spectral Galerkin approximation in $V_{\mathcal{N}}$. The result follows from the triangle inequality

$$\|u - \tilde{u}_{\mathcal{N}}\|_1 \leq \|u - u_{\mathcal{N}}\|_1 + \|u_{\mathcal{N}} - \tilde{u}_{\mathcal{N}}\|_1, \tag{16}$$

the estimate from spectral approximation [9]

$$\|u - u_{\mathcal{N}}\|_1 \leq C\beta_{\mathcal{N}}^{-1} \inf_{w \in V_{\mathcal{N}}} \|u - w\|_1 \tag{17}$$

and the convergence rate for greedy algorithm [10]

$$\|u_{\mathcal{N}} - \tilde{u}_{\mathcal{N}}\|_1 \leq Ce^{-\eta N}. \tag{18}$$

□

5 Numerical Results

In this section, we applied the HMABS method to several numerical examples to demonstrate the feasibility and the efficiency. We compared the HMABS method with both the traditional homotopy method and the bootstrapping method. The discretized polynomial systems solved by the homotopy method were based on 20 grid points for 1D examples and 5×5 grid points for 2D examples. The stopping criteria of the bootstraping method was based on the step size, namely, $h < 10^{-3}$ in 1D and $h_x < 10^{-2}$ and $h_y < 10^{-2}$ in 2D while the stopping criteria of the HMABS approach was $\varepsilon < 10^{-3}$ in Eq. (11) with $\mathcal{N} = 100$. The residual errors reported in this section were computed by taking the maximum value of the residual of Eq. (5) evaluated by the numerical solution and different basis functions. All experiments were run on a cluster consisting of a manager that uses one core of a Xeon 5410 processor and up to 10 computing nodes, each containing two Xeon 5410 processors running 64-bit Linux, i.e., each node consists of 8 processing cores. Comparisons of all the algorithms were implemented on Matlab incorporated with the homotopy tracking package in Bertini [7].

Table 1 Summary of solutions for example (19)

The HMABS method		The spectral method	
Basis	L^2 error	Basis	L^2 error
$\{\phi^1\}$	2.7806	$\{\phi^1\}$	2.7806
$\{\phi^1, \phi^3\}$	5.7005e−2	$\{\phi^1, \phi^2\}$	2.7817
$\{\phi^1, \phi^3, \phi^5\}$	6.2725e−4	$\{\phi^1, \phi^2, \phi^3\}$	5.7918e−2
$\{\phi^1, \phi^3, \phi^5, \phi^7\}$	4.3018e−6	$\{\phi^1, \phi^2, \phi^3, \phi^4\}$	5.7821e−2
$\{\phi^1, \phi^3, \phi^5, \phi^7, \phi^9\}$	3.1736e−8	$\{\phi^1, \phi^2, \phi^3, \phi^4, \phi^5\}$	6.2516e−4
$\{\phi^1, \phi^3, \phi^5, \phi^7, \phi^9, \phi^{11}\}$	2.1938e−10	$\{\phi^1, \phi^2, \phi^3, \phi^4, \phi^5, \phi^6\}$	6.2273e−4

5.1 A 1D Example with One Exact Solution

We first verified the accuracy of the HMABS method by considering the following one dimensional problem,

$$\begin{cases} -u_{xx} + u^2 = \pi^2 \sin(x) + \sin(\pi x)^2 & \text{in } \Omega = (0, 1), \\ u(0) = u(1) = 0, \end{cases} \tag{19}$$

which has an exact solution $u(x) = \sin(\pi x)$. In the HMABS method, we chose the following basis functions

$$\phi_i(x) = \frac{x^{i+2} - t}{i^2 + 3i + 2}, \quad i = 0, 1, 2, \ldots, \mathcal{N},$$

which satisfies

$$-(\phi_i)_{xx} = x^i \text{ in } \Omega, \quad \phi_i = 0 \text{ on } \partial\Omega.$$

Since (19) has a unique solution, we use Newton's method to compute the discretized polynomial system instead of homotopy method. In Table 1, we compared the L^2 error of HMABS method with the spectral discretization. It clearly shows that the HMABS method selects the odd basis only which is consistent with the polynomial expansion of the exact solution. The L^2 errors reported in Table 1 shows the spectral accuracy of the HMABS method which is better than that of the traditional spectral method.

5.2 A 1D Example with Two Solutions

Secondly, we considered the following 1D example with two analytical solutions [33]

$$\begin{cases} u_{xx} = -\lambda(1 + u^4) & \text{on } (0, 1), \\ u'(0) = u(1) = 0, \end{cases} \tag{20}$$

where $\lambda \in R^+$ is a parameter. Multiplying by u_x and integrating over $[0, x]$ on Eq. (20), we obtained

$$\frac{1}{2}(u_x)^2 + F(u) - F(u_0) = 0, \tag{21}$$

Table 2 Summary of solutions

λ	Basis	L^2 error		Residual	
		1st sol.	2nd sol.	1st sol.	2nd sol.
1	$\{\phi^0\}$	1.34e−2	6.79e−1	3.16e−2	1.26
	$\{\phi^0, \phi^1\}$	6.43e−4	4.78e−2	3.75e−3	1.43e−1
	$\{\phi^0, \phi^1, \phi^4\}$	2.49e−4	4.73e−3	3.23e−3	7.06e−2
	$\{\phi^0, \phi^1, \phi^4, \phi^{15}\}$	2.12e−4	4.80e−3	4.24e−4	8.14e−2
	$\{\phi^0, \phi^1, \phi^4, \phi^{15}, \phi^2\}$	9.15e−5	2.53e−3	2.58e−5	2.72e−2
	$\{\phi^0, \phi^1, \phi^4, \phi^{15}, \phi^2, \phi^8\}$	8.44e−5	7.88e−4	8.32e−6	2.23e−3
	$\{\phi^0, \phi^1, \phi^4, \phi^{15}, \phi^2, \phi^8, \phi^{20}\}$	8.42e−5	4.54e−4	3.52e−7	1.61e−3
1.2	$\{\phi^0\}$	5.26e−2	5.03e−1	1.01e−1	8.04e−1
	$\{\phi^0, \phi^1\}$	2.30e−3	2.56e−2	1.40e−3	6.14e−2
	$\{\phi^0, \phi^1, \phi^4\}$	7.49e−4	3.40e−3	1.19e−2	6.73e−2
	$\{\phi^0, \phi^1, \phi^4, \phi^2\}$	3.36e−4	2.51e−3	3.74e−3	3.22e−2
	$\{\phi^0, \phi^1, \phi^4, \phi^2, \phi^{14}\}$	2.18e−4	1.27e−3	1.43e−4	4.40e−3
	$\{\phi^0, \phi^1, \phi^4, \phi^2, \phi^{14}, \phi^8\}$	1.84e−4	3.95e−4	4.20e−5	8.35e−4

where $F(u) = \int_0^u \lambda(1 + s^p)ds$ and $u_0 = u(0)$. Since $u_x < 0$ for $x > 0$, we have

$$\int_0^{u(x)} \frac{ds}{\sqrt{F(u_0) - F(s)}} = \sqrt{2}(1 - x). \tag{22}$$

There exists two solutions for $\lambda < \lambda^* \approx 1.30107$ [33]. Thus the exact solutions can be obtained from (22) and compared with numerical solutions. The basis functions were chosen as

$$\phi_i(x) = \frac{x^{i+2} - 1}{i^2 + 3i + 2}, \quad i = 0, 1, 2, \ldots, \mathcal{N},$$

which satisfies

$$\begin{cases} (\phi_i)_{xx} = x^i \quad \text{on } (0, 1), \\ \phi_i'(0) = \phi_i(1) = 0. \end{cases} \tag{23}$$

Table 2 shows the L^2 error and residual of the two numerical solutions obtained by the HMABS method for $\lambda = 1$ and $\lambda = 1.2$ respectively. We can clearly see that the HMABS method converges in about 6–7 iterations and then the size of discretized polynomial systems are much smaller.

5.3 A 1D Example With Multiple Solutions

Next, we considered the following parametric example with multiple solutions,

$$\begin{cases} u_{xx} = -\frac{\pi^2}{4}u^2(u^2 - p) \quad \text{on } (0, 1), \\ u'(0) = u(1) = 0, \end{cases} \tag{24}$$

where $p \in R^+$ is a parameter [13]. For this parametric problem, the number of solutions increases as p increases. In particular, the solutions' behavior of (24) is shown in Fig. 1.

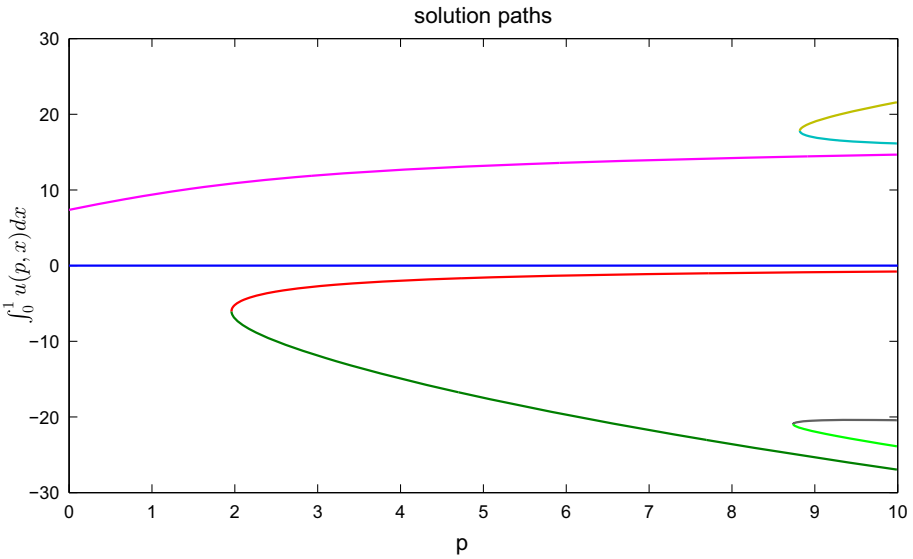

Fig. 1 Solutions' behavior of (20): the solutions are projected by integrating x. When p is fixed, the number of intersections represents the number of solutions of (20)

Table 3 Summary of solutions

p	Basis	Residual	# Solns
1	$\{\phi^0\}$	0.03182	2
	$\{\phi^0, \phi^1\}$	0.00225	2
	$\{\phi^0, \phi^1, \phi^4\}$	0.00014	2
8	$\{\phi^0\}$	0.61781	4
	$\{\phi^0, \phi^1\}$	0.14805	6
	$\{\phi^0, \phi^1, \phi^4\}$	0.02458	6
	$\{\phi^0, \phi^1, \phi^4, \phi^{11}\}$	0.00212	4
	$\{\phi^0, \phi^1, \phi^4, \phi^{11}, \phi^2\}$	0.00039	4
10	$\{\phi^0\}$	0.96285	4
	$\{\phi^0, \phi^1\}$	0.62123	8
	$\{\phi^0, \phi^1, \phi^5\}$	0.30865	16
	$\{\phi^0, \phi^1, \phi^5, \phi^2\}$	0.02243	10
	$\{\phi^0, \phi^1, \phi^5, \phi^2, \phi^{17}\}$	0.00395	8
	$\{\phi^0, \phi^1, \phi^5, \phi^2, \phi^{17}, \phi^9\}$	0.00041	8

In [33], the shooting method was utilized to numerically confirm the number of solutions of (20). In this example, we chose the same basis functions $\{\phi_i\}_{i=0}^{\mathcal{N}}$ as the previous example. Table 3 shows that the HMABS method produces the same number of solutions as the shooting method. From Table 4, we can see that the HMABS method is much more efficient than the traditional homotopy continuation and the bootstrapping method for computing the same number of solutions.

Table 4 Computing time comparisons of different methods

p	HMABS	Bootstrapping	Homotopy
1	3m26s	1h39m	1d12h
8	8m12s	3h20m	1d12h
10	10m30s	5h41m	1d12h

Table 5 Numerical results of Example (25)

p	Basis	Residual	# Solns
800	$\{\phi^{1,1}\}$	10.293	1
	$\{\phi^{1,1}, \phi^{1,4}\}$	4.6146	2
	$\{\phi^{1,1}, \phi^{1,4}, \phi^{1,2}\}$	0.2832	6
	$\{\phi^{1,1}, \phi^{1,4}, \phi^{1,2}, \phi^{2,1}\}$	0.0092	8
	$\{\phi^{1,1}, \phi^{1,4}, \phi^{1,2}, \phi^{2,1}, \phi^{2,2}\}$	2.2737e−3	10
	$\{\phi^{1,1}, \phi^{1,4}, \phi^{1,2}, \phi^{2,1}, \phi^{4,1}\}$	4.2839e−6	10
3000	$\{\phi^{1,1}\}$	75.0182	1
	$\{\phi^{1,1}, \phi^{1,2}\}$	19.4927	4
	$\{\phi^{1,1}, \phi^{1,2}, \phi^{2,1}\}$	1.0408	6
	$\{\phi^{1,1}, \phi^{1,2}, \phi^{2,1}, \phi^{1,3}\}$	0.2319	8
	$\{\phi^{1,1}, \phi^{1,2}, \phi^{2,1}, \phi^{1,3}, \phi^{3,1}\}$	0.1038	18
	$\{\phi^{1,1}, \phi^{1,2}, \phi^{2,1}, \phi^{1,3}, \phi^{3,1}, \phi^{3,2}\}$	0.0361	22
	$\{\phi^{1,1}, \phi^{1,2}, \phi^{2,1}, \phi^{1,3}, \phi^{3,1}, \phi^{3,2}, \phi^{2,3}\}$	1.8245e−3	18
	$\{\phi^{1,1}, \phi^{1,2}, \phi^{2,1}, \phi^{1,3}, \phi^{3,1}, \phi^{3,2}, \phi^{3,4}\}$	1.7405e−4	18
5000	$\{\phi^{1,1}\}$	120.3827	1
	$\{\phi^{1,1}, \phi^{1,2}\}$	50.2736	4
	$\{\phi^{1,1}, \phi^{1,2}, \phi^{2,1}\}$	10.3746	6
	$\{\phi^{1,1}, \phi^{1,2}, \phi^{2,1}, \phi^{1,3}\}$	0.9763	14
	$\{\phi^{1,1}, \phi^{1,2}, \phi^{2,1}, \phi^{1,3}, \phi^{3,1}\}$	0.1846	24
	$\{\phi^{1,1}, \phi^{1,2}, \phi^{2,1}, \phi^{1,3}, \phi^{3,1}, \phi^{3,2}\}$	0.0518	46
	$\{\phi^{1,1}, \phi^{1,2}, \phi^{2,1}, \phi^{1,3}, \phi^{3,1}, \phi^{3,2}, \phi^{2,3}\}$	0.0183	34
	$\{\phi^{1,1}, \phi^{1,2}, \phi^{2,1}, \phi^{1,3}, \phi^{3,1}, \phi^{3,2}, \phi^{3,4}\}$	5.2831e−3	30
	$\{\phi^{1,1}, \phi^{1,2}, \phi^{2,1}, \phi^{1,3}, \phi^{3,1}, \phi^{3,2}, \phi^{3,4}, \phi^{4,3}\}$	9.2836e−4	30

5.4 Verifying the Breuera–McKennab Conjecture in 2D

We applied the HMABS method to the Breuera–McKennab conjecture with multiple solutions that have been studied in [12]:

$$\begin{cases} -\Delta u = u^2 - p\sin(\pi x)\sin(\pi y) & \text{in } \Omega = (0,1)\times(0,1), \\ u = 0 & \text{on } \partial\Omega. \end{cases} \tag{25}$$

Table 6 Computing time comparison for example (25)

p	HMABS	Bootstrapping
800	28m12s	39h45m
3000	30m24s	59h42m
5000	42m9s	71h13m

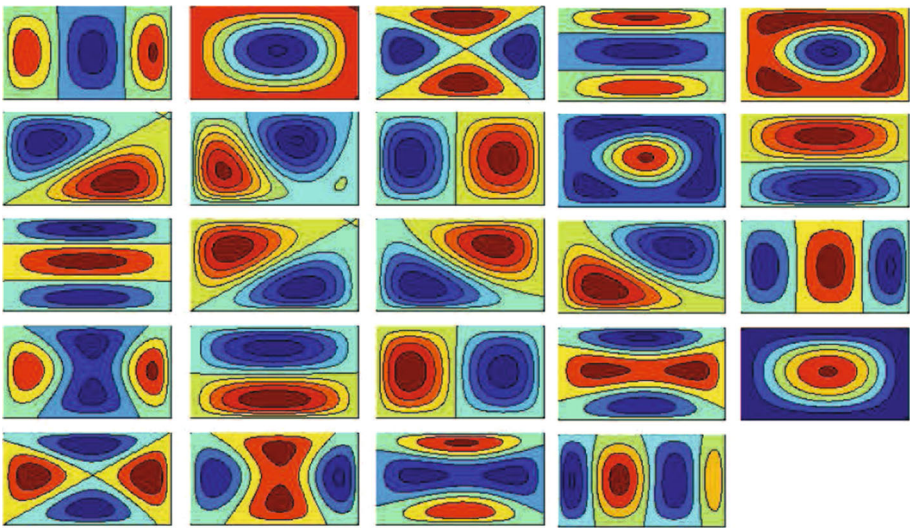

Fig. 2 The contours of the solutions to (27)

The HMABS method solved the Breuera–McKennab conjecture for different parameter p with the basis functions $\{\phi_{i,j}(x, y)\}$ by solving the following linear differential equations:

$$\begin{cases} -\Delta\phi_{i,j} = x^i y^j & \text{in } \Omega = (0,1) \times (0,1), \\ \phi_{i,j} = 0 & \text{on } \partial\Omega. \end{cases} . \tag{26}$$

The number of multiple solutions computed by the HMABS method for $p = 800, 3000$ and 5000 is listed in Table 5 which coincides with those reported in [2,61]. Table 6 illustrates the efficiency of the HMABS method when comparing with the bootstrapping method.

5.5 The Henon Equation in 2D

We also tested the HMABS method on the Henon equation [62] with $r = 0$ and $q = 3$, namely,

$$\begin{cases} -\Delta u = u^3 & \text{in } \Omega = (0,1) \times (0,1), \\ u = 0 & \text{on } \partial\Omega. \end{cases} . \tag{27}$$

The basis functions $\{\phi_{i,j}(x, y)\}$ of the HMABS method are the same as those of the previous example. The first eight solutions of (27) have been computed numerically in [62]. The HMABS method found 24 solutions shown in Fig. 2. The number of solutions with different subspaces are listed in Table 7. The HMABS method is competitive with the method based on numerical optimization present in [62]: although some of solutions shown in [62] are

Table 7 Summary of solutions for example (27)

Basis	Residual	# Solns
$\{\phi^{1,1}\}$	0.04565	3
$\{\phi^{1,1}, \phi^{2,3}\}$	0.00889	5
$\{\phi^{1,1}, \phi^{2,3}, \phi^{1,4}\}$	0.00242	7
$\{\phi^{1,1}, \phi^{2,3}, \phi^{1,4}, \phi^{4,1}\}$	0.00168	11
$\{\phi^{1,1}, \phi^{2,3}, \phi^{1,4}, \phi^{4,1}, \phi^{3,2}\}$	5.6212e−4	14
$\{\phi^{1,1}, \phi^{2,3}, \phi^{1,4}, \phi^{4,1}, \phi^{3,2}, \phi^{1,3}\}$	1.3821e−4	20
$\{\phi^{1,1}, \phi^{2,3}, \phi^{1,4}, \phi^{4,1}, \phi^{3,2}, \phi^{1,3}, \phi^{3,1}\}$	8.0121e−5	24
$\{\phi^{1,1}, \phi^{2,3}, \phi^{1,4}, \phi^{4,1}, \phi^{3,2}, \phi^{1,3}, \phi^{3,1}, \phi^{4,4}\}$	4.8340e−5	24

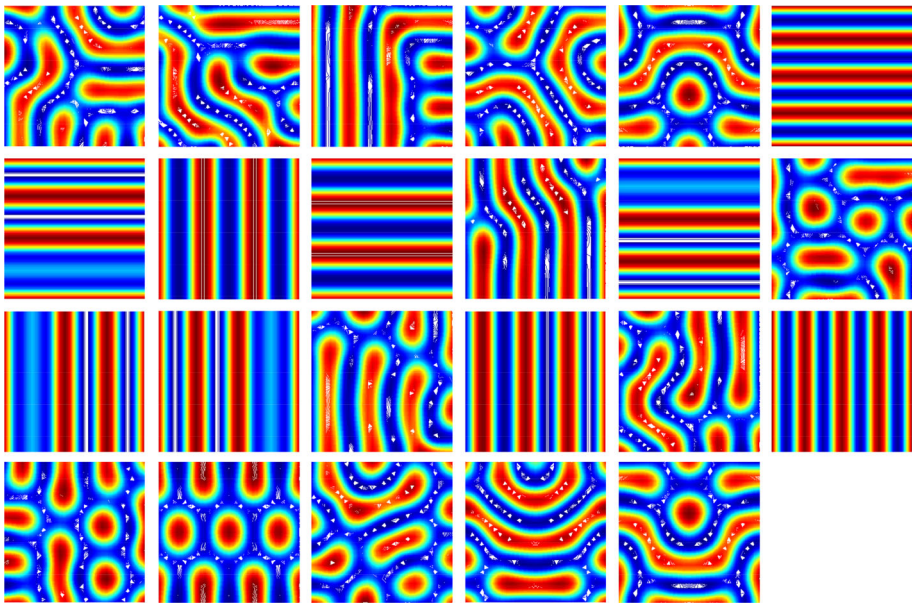

Fig. 3 Stable steady state solutions for the 2D Gray–Scott model ($d_A = d_S = 0.1$, $\rho = 0.05$, and $k = 0.2$)

missed by the HMABS method, some unknown solutions are founded by introducing only 8 basis.

5.6 Applications in Pattern Formation Problems

Last, we applied the HMABS method to the pattern formation problem which is one of the fundamental questions in mathematical biology, namely, how multiple patterns and different solution structures can be computed efficiently for nonlinear biological models. The HMABS method provides a new approach to obtain the multiple patterns in this direction. In order to demonstrate the idea, we will use the Gray–Scott model [44] as an example: two reactions $A+2S \rightarrow 3S$ and $S \rightarrow P$. Both reactions are irreversible, P is called an inert product [58]. A nonequilibrium constraint is represented by a feeding term for A. Both A and S are removed

Table 8 Iteration details of the HMABS method and comparisons with other methods for the Gray–Scott model with different ρ and k ($d_A = d_S = 0.1$). The table shows the selected basis functions for every iteration

(ρ, k)	Basis	Residual	# Solns
(0.2, 0.95)	$\{\phi^{1,1}\}$	10.293	2
	$\{\phi^{1,1}, \phi^{1,4}\}$	0.0827	4
	$\{\phi^{1,1}, \phi^{1,4}, \phi^{1,2}\}$	0.00225	7
	$\{\phi^{1,1}, \phi^{1,4}, \phi^{1,2}, \phi^{2,1}\}$	6.4739e−5	11
	$\{\phi^{1,1}, \phi^{1,4}, \phi^{1,2}, \phi^{2,1}, \phi^{4,1}\}$	4.2839e−7	11
(0.35, 0.5)	$\{\phi^{1,1}\}$	75.0182	1
	$\{\phi^{1,1}, \phi^{2,1}\}$	1.0408	6
	$\{\phi^{1,1}, \phi^{2,1}, \phi^{1,3}\}$	0.5746	11
	$\{\phi^{1,1}, \phi^{2,1}, \phi^{1,3}, \phi^{3,1}\}$	0.1038	15
	$\{\phi^{1,1}, \phi^{2,1}, \phi^{1,3}, \phi^{3,1}, \phi^{3,1}\}$	3.8373e−3	18
	$\{\phi^{1,1}, \phi^{2,1}, \phi^{1,3}, \phi^{3,1}, \phi^{3,1}, \phi^{3,2}\}$	3.6112e−5	20
	$\{\phi^{1,1}, \phi^{2,1}, \phi^{1,3}, \phi^{3,1}, \phi^{3,1}, \phi^{3,2}, \phi^{3,4}, \}$	2.8373e−6	15
	$\{\phi^{1,1}, \phi^{2,1}, \phi^{1,3}, \phi^{3,1}, \phi^{3,1}, \phi^{3,2}, \phi^{3,4}, \phi^{4,3}\}$	1.7405e−7	15
(0.05, 0.2)	$\{\phi^{1,1}\}$	120.3827	1
	$\{\phi^{1,1}, \phi^{1,2}\}$	50.8272	3
	$\{\phi^{1,1}, \phi^{1,2}, \phi^{2,1}\}$	10.3746	6
	$\{\phi^{1,1}, \phi^{1,2}, \phi^{2,1}, \phi^{1,3}\}$	1.2834	12
	$\{\phi^{1,1}, \phi^{1,2}, \phi^{2,1}, \phi^{1,3}, \phi^{3,1}\}$	0.1846	20
	$\{\phi^{1,1}, \phi^{1,2}, \phi^{2,1}, \phi^{1,3}, \phi^{3,1}, \phi^{3,2}\}$	0.0518	24
	$\{\phi^{1,1}, \phi^{1,2}, \phi^{2,1}, \phi^{1,3}, \phi^{3,1}, \phi^{3,2}, \phi^{2,3}\}$	0.0183	27
	$\{\phi^{1,1}, \phi^{1,2}, \phi^{2,1}, \phi^{1,3}, \phi^{3,1}, \phi^{3,2}, \phi^{2,3}, \phi^{3,4}\}$	5.2726e−3	25
	$\{\phi^{1,1}, \phi^{1,2}, \phi^{2,1}, \phi^{1,3}, \phi^{3,1}, \phi^{3,2}, \phi^{2,3}, \phi^{3,4}, \phi^{4,3}\}$	9.2836e−4	23
	$\{\phi^{1,1}, \phi^{1,2}, \phi^{2,1}, \phi^{1,3}, \phi^{3,1}, \phi^{3,2}, \phi^{2,3}, \phi^{3,4}, \phi^{4,3}, \phi^{1,4}\}$	3.6252e−5	23
	$\{\phi^{1,1}, \phi^{1,2}, \phi^{2,1}, \phi^{1,3}, \phi^{3,1}, \phi^{3,2}, \phi^{2,3}, \phi^{3,4}, \phi^{4,3}, \phi^{1,4}, \phi^{4,1}\}$	9.2836e−7	23

by the feed process [58]. The resulting reaction-diffusion equations in dimensionless units with no-flux boundary conditions are [44]:

$$\begin{cases} \frac{\partial A}{\partial t} = d_A \Delta A - S^2 A + \rho(1 - A), \\ \frac{\partial S}{\partial t} = d_S \Delta S + S^2 A - (\rho + k) S. \end{cases} \tag{28}$$

This model describes the growth of an activator A reacted with substrate S fed from the activator with a rate ρ, and S is converted to an inert product at the rate k. d_A and d_S are the diffusion coefficients of A and S, respectively.

We applied the HMABS method to solve the steady state system of the Gray–Scott model with $d_A = d_S = 0.1$, $\rho = 0.05$, and $k = 0.2$ in 2D. The stable steady states are shown in Fig. 3. The results of different ρ and k are shown in Table 8. In this example, the HMABS method is also compared with the homotopy method and the bootstrapping method and shows the computational efficiency with less computing time in Table 6.

Table 9 Computing time Comparison of HMABS with other methods

(ρ, κ)	HRBM	Homotopy	Bootstrapping
(0.2, 0.95)	8m23s	4d21h	4h12m
(0.35, 0.5)	21m23s	4d21h	12h19m
(0.05, 0.2)	30m34s	4d21h	1d1h

6 Conclusion

A homotopy method with adaptive basis selection has been developed to solve nonlinear differential equation with multiple solutions. *The idea is to choose optimal basis functions to minimize the size of the discretized polynomial system. A new homotopy continuation method is designed to efficiently solve this discretized polynomial system.* The convergence of the proposed method has also been discussed. We tested several 1D and 2D examples to demonstrate the efficiency of the HMABS method. The computations in 3D shall be considered in the future along with a detailed analysis of how to choose an optimal set of basis functions (Table 9).

Acknowledgements W. Hao's research was supported by the American Heart Association (Grant 17SDG33660722) and National Science Foundation (Grant DMS-1818769). GL would like to gratefully acknowledge the support from National Science Foundation (DMS-1555072, DMS-1736364 and DMS-1821233). B. Zheng would like to acknowledge the support by Beijing Institute for Scientific and Engineering Computing and by the U.S. Department of Energy, Office of Science, Office of Advanced Scientific Computing Research, Applied Mathematics program as part of the Collaboratory on Mathematics for Mesoscopic Modeling of Materials and a Laboratory Directed Research and Development (LDRD) Program from Pacific Northwest National Laboratory. The PNNL is operated by Battelle for the US Department of Energy under Contract DE-AC05-76RL01830.

References

1. Allgower, E., Bates, D., Sommese, A., Wampler, C.: Solution of polynomial systems derived from differential equations. Computing **76**(1–2), 1–10 (2006)
2. Allgower, E., Cruceanu, S., Tavener, S.: Application of numerical continuation to compute all solutions of semilinear elliptic equations. Adv. Geom. **9**(3), 371–400 (2009)
3. Bates, D., Hauenstein, J., Sommese, A., Wampler, C.: Adaptive multiprecision path tracking. SIAM J. Numer. Anal. **46**(2), 722–746 (2008)
4. Bates, D., Hauenstein, J., Sommese, A., Wampler, C.: Stepsize control for path tracking. Contemp. Math. **496**(3), 21–31 (2009)
5. Bates, D., Hauenstein, J., Sommese, A., Wampler, C.: Numerically Solving Polynomial Systems with Bertini, vol. 25. SIAM, Philadelphia (2013)
6. Bates, D.J., Hauenstein, J.D., Sommese, A.J., Wampler, C.W.: Adaptive multiprecision path tracking. SIAM J. Nume. Anal. **46**(2), 722–746 (2008)
7. Bates, D.J., Hauenstein, J.D., Sommese, A.J., Wampler, C.W.: Numerically Solving Polynomial Systems with Bertini, vol. 25. SIAM, Philadelphia (2013)
8. Bauer, L., Keller, H.B., Reiss, E.: Multiple eigenvalues lead to secondary bifurcation. SIAM Rev. **17**(1), 101–122 (1975)
9. Bernardi, C., Maday, Y.: Spectral methods. Handb. Numer. Anal. **5**, 209–485 (1997)
10. Binev, P., Cohen, A., Dahmen, W., DeVore, R., Petrova, G., Wojtaszczyk, P.: Convergence rates for greedy algorithms in reduced basis methods. SIAM J. Math. Anal. **43**, 1457–1472 (2011)
11. Braun, M., Golubitsky, M.: Differential Equations and Their Applications, vol. 4. Springer, New York (1983)
12. Breuer, B., McKenna, P., Plum, M.: Multiple solutions for a semilinear boundary value problem: a computational multiplicity proof. J. Differ. Equ. **195**(1), 243–269 (2003)

13. Chen, C., Xie, Z.: Structure of multiple solutions for nonlinear differential equations. Sci. China Ser. A Math. **47**(1), 172–180 (2004)
14. Chen, F., Shen, J., Yu, H.: A new spectral element method for pricing european options under the black-scholes and merton jump diffusion models. J. Sci. Comput. **52**(3), 499–518 (2012)
15. Chen, Y., Hesthaven, J., Maday, Y., Rodrguez, J.: Improved successive constraint method based a posteriori error estimate for reduced basis approximation of 2D Maxwell's problem. ESAIM Math. Model. Numer. Anal. **43**(6), 1099–1116 (2009)
16. Chen, Y., Hesthaven, J.S., Maday, Y., Rodríguez, J.: Certified reduced basis methods and output bounds for the harmonic Maxwell's equations. SIAM J. Sci. Comput. **32**(2), 970–996 (2010)
17. Chossat, P., Golubitsky, M.: Symmetry-increasing bifurcation of chaotic attractors. Physica D **32**(3), 423–436 (1988)
18. Cristini, V., Li, X., Lowengrub, J., Wise, S.: Nonlinear simulations of solid tumor growth using a mixture model: invasion and branching. J. Math. Biol. **58**(4), 723–763 (2009)
19. Cristini, V., Lowengrub, J., Nie, Q.: Nonlinear simulation of tumor growth. J. Math. Biol. **46**(3), 191–224 (2003)
20. Fontelos, M., Friedman, A.: Symmetry-breaking bifurcations of free boundary problems in three dimensions. Asymptot. Anal. **35**(3), 187–206 (2003)
21. Friedman, A.: Free boundary problems in biology. Philos. Trans. R. Soc. A **373**(2050), 20140368 (2015)
22. Friedman, A., Hao, W.: A mathematical model of atherosclerosis with reverse cholesterol transport and associated risk factors. Bull. Math. Biol. **77**(5), 758–781 (2015)
23. Friedman, A., Hu, B.: Bifurcation from stability to instability for a free boundary problem arising in a tumor model. Arch. Ration. Mech. Anal. **180**(2), 293–330 (2006)
24. Friedman, A., Hu, B.: Bifurcation for a free boundary problem modeling tumor growth by Stokes equation. SIAM J. Math. Anal. **39**(1), 174–194 (2007)
25. Friedman, A., Reitich, F.: Symmetry-breaking bifurcation of analytic solutions to free boundary problems: an application to a model of tumor growth. Trans. Am. Math. Soc. **353**(4), 1587–1634 (2001)
26. Golubitsky, M., Stewart, I.: The Symmetry Perspective: From Equilibrium to Chaos in Phase Space and Physical Space, vol. 200. Springer, New York (2003)
27. Golubitsky, M., Stewart, I.: Singularities and Groups in Bifurcation Theory, vol. 2. Springer, New York (2012)
28. Grepl, M., Patera, A.: A posteriori error bounds for reduced-basis approximations of parametrized parabolic partial differential equations. ESAIM Math. Model. Numer. Anal. **39**(1), 157–181 (2005)
29. Haber, R., Unbehauen, H.: Structure identification of nonlinear dynamic systems survey on input/output approaches. Automatica **26**(4), 651–677 (1990)
30. Hao, W., Crouser, E., Friedman, A.: Mathematical model of sarcoidosis. Proc. Nat. Acad. Sci. **111**(45), 16065–16070 (2014)
31. Hao, W., Friedman, A.: The ldl-hdl profile determines the risk of atherosclerosis: a mathematical model. PLoS ONE **9**(3), e90497 (2014)
32. Hao, W., Hauenstein, J., Hu, B., Liu, Y., Sommese, A., Zhang, Y.-T.: Bifurcation for a free boundary problem modeling the growth of a tumor with a necrotic core. Nonlinear Anal. Real World Appl. **13**(2), 694–709 (2012)
33. Hao, W., Hauenstein, J., Hu, B., Sommese, A.: A bootstrapping approach for computing multiple solutions of differential equations. J. Comput. Appl. Math. **258**, 181–190 (2014)
34. Hao, W., Hauenstein, J., Shu, C.-W., Sommese, A., Xu, Z., Zhang, Y.-T.: A homotopy method based on weno schemes for solving steady state problems of hyperbolic conservation laws. J. Comput. Phys. **250**, 332–346 (2013)
35. Hao, W., Nepomechie, R., Sommese, A.: Completeness of solutions of bethe's equations. Phys. Rev. E **88**(5), 052113 (2013)
36. Hao, W., Nepomechie, R., Sommese, A.: Singular solutions, repeated roots and completeness for higher-spin chains. J. Stat. Mech Theory Exp. **2014**(3), P03024 (2014)
37. Hao, W., Sommese, A., Zeng, Z.: Algorithm 931: an algorithm and software for computing multiplicity structures at zeros of nonlinear systems. ACM Trans. Math. Softw. TOMS **40**(1), 5–20 (2013)
38. Hou, T., Lowengrub, J., Shelley, M.: Boundary integral methods for multicomponent fluids and multiphase materials. J. Comput. Phys. **169**(2), 302–362 (2001)
39. Li, T.-Y., Sauer, T., Yorke, J.: The Cheater's homotopy: an efficient procedure for solving systems of polynomial equations. SIAM J. Numer. Anal. **26**(5), 1241–1251 (1989)
40. Li, T.-Y., Zeng, Z.: Homotopy-determinant algorithm for solving nonsymmetric eigenvalue problems. Math. Comput. **59**(200), 483–502 (1992)
41. Morgan, A., Sommese, A.: Computing all solutions to polynomial systems using homotopy continuation. Appl. Math. Comput. **24**(2), 115–138 (1987)

42. Morgan, A., Sommese, A.: A homotopy for solving general polynomial systems that respects m-homogeneous structures. Appl. Math. Comput. **24**(2), 101–113 (1987)
43. Peaceman, D., Rachford, H.: The numerical solution of parabolic and elliptic differential equations. J. Soc. Ind. Appl. Math. **3**(1), 28–41 (1955)
44. Pearson, J.: Complex patterns in a simple system. Science **261**(3), 189–189 (1993)
45. Pousin, J., Rappaz, J.: Consistency, stability, a priori and a posteriori errors for petrov-galerkin methods applied to nonlinear problems. Numer. Math. **69**(2), 213–231 (1994)
46. Rabier, P., Rheinboldt, W.: On a computational method for the second fundamental tensor and its application to bifurcation problems. Numer. Math. **57**(1), 681–694 (1990)
47. Rheinboldt, W.: Numerical methods for a class of finite dimensional bifurcation problems. SIAM J. Numer. Anal. **15**(1), 1–11 (1978)
48. Rheinboldt, W.: Numerical analysis of continuation methods for nonlinear structural problems. Comput. Struct. **13**(1), 103–113 (1981)
49. Rheinboldt, W., Burkardt, J.: A locally parameterized continuation process. ACM Trans. Math. Softw. TOMS **9**(2), 215–235 (1983)
50. Rozza, G., Huynh, D., Patera, A.: Reduced basis approximation and a posteriori error estimation for affinely parametrized elliptic coercive partial differential equations. Arch. Comput. Methods Eng. **15**(3), 1 (2007)
51. Rozza, G., Huynh, D., Patera, A.: Reduced basis approximation and a posteriori error estimation for affinely parametrized elliptic coercive partial differential equations. Arch. Comput. Methods Eng. **15**(3), 229–275 (2008)
52. Shen, J., Tang, T., Wang, L.: Spectral Methods: Algorithms, Analysis and Applications, vol. 41. Springer, New York (2011)
53. Smith, G.: Numerical Solution of Partial Differential Equations: Finite Difference Methods. Oxford University Press, Oxford (1985)
54. Sommese, A., Verschelde, J., Wampler, C.: Homotopies for intersecting solution components of polynomial systems. SIAM J. Numer. Anal. **42**(4), 1552–1571 (2004)
55. Sommese, A., Verschelde, J., Wampler, C.: An intrinsic homotopy for intersecting algebraic varieties. J. Complex. **21**(4), 593–608 (2005)
56. Sommese, A., Wampler, C.: The Numerical Solution of Systems of Polynomials Arising in Engineering and Science, vol. 99. World Scientific, Singapore (2005)
57. Strogatz, S.: Nonlinear Dynamics and Chaos: With Applications to Physics, Biology, Chemistry, and Engineering. Westview press, Boulder (2014)
58. Turton, R., Bailie, R., Whiting, W., Shaeiwitz, J.: Analysis, Synthesis and Design of Chemical Processes. Pearson Education, London (2008)
59. Veroy, K., Prud'Homme, C., Rovas, D., Patera, A.: A posteriori error bounds for reduced-basis approximation of parametrized noncoercive and nonlinear elliptic partial differential equations. In: 16th AIAA Computational Fluid Dynamics Conference, p. 3847 (2003)
60. Xu, J.: Two-grid discretization techniques for linear and nonlinear pdes. SIAM J. Numer. Anal. **33**(5), 1759–1777 (1996)
61. Zhang, X., Zhang, J., Yu, B.: Eigenfunction expansion method for multiple solutions of semilinear elliptic equations with polynomial nonlinearity. SIAM J. Numer. Anal. **51**(5), 2680–2699 (2013)
62. Zhou, J.: Solving multiple solution problems: computational methods and theory revisited. Commun. Appl. Math. **3**(1), 1–31 (2017)